Supporting Information

One stone, two birds: high efficiency blue emitting perovskite nanocrystals for LED and security ink applications

Chun Sun,*,† Zhiyuan Gao,† Hanxin Liu,† Le Wang,† Yuchen Deng,‡ Peng Li,‡ Huanrong Li,‡ Zi-Hui Zhang,† Chao Fan,† and Wengang Bi*,†

† State Key Laboratory of Reliability and Intelligence of Electrical Equipment, Hebei University of Technology, 5340 Xiping Road, Tianjin, 300401, P. R. China

Tianjin Key Laboratory of Electronic Materials and Devices, School of Electronics and Information Engineering, Hebei University of Technology, 5340 Xiping Road, Tianjin, 300401, P. R. China

‡ Hebei Provincial Key Lab of Green Chemical Technology and High Efficient Energy Saving, School of Chemical Engineering and Technology, Hebei University of Technology, Tianjin 300130, P. R. China

Calculation of the molar ratio:

The concentrations of 3D and 0D perovskite are 0.5mg/mL and 0.2mg/mL, respectively. The weight of a single NC can be calculated using the formula,
$m = \rho \times V$,
where m is the mass of each NC, ρ is the density of perovskite (bulk $CsPbCl_3$ =4.24 g cm^{-3} and bulk Cs_4PbBr_6 =4.299 g cm^{-3})[1, 2], and V is the volume of a NC.
Considering the cube shape of 3D NCs, the volume of $CsPbCl_3$ NC can be calculated as,
$V = a^3$,
where a is the average edge-length (8.5nm) of a NC obtained from TEM.
The Cs_4PbBr_6 NC can be treated as near-spherical particles, whose volume can be calculated as $V = 4/3*\pi r^3$ (r= the radius (11nm) of a NC obtained from TEM).
For 50uL NC solution, the number of NCs (N) in the sample can be obtained as below,
$N=M/m$,
where M is the weight of the NC sample (for $CsPbCl_3$, M= 0.05*0.5=0.025mg and for Cs_4PbBr_6, M=0.05*0.2=0.01mg), m is the weight of a single NC.
This number of NCs is then converted to a mole of NCs by dividing with Avogadro's number (N_A). In the end, the mole numbers of 50 uL 3D and 0 D perovskite are $1.6*10^{-11}$ mol and $0.7*10^{-12}$ mol, respectively. The molar ratio of 50 uL 0D and 3 D perovskite should be 0.04:1, which corresponding to the $Cs_4PbBr_6/CsPbCl_3$ volume ratio of 1:1. The rest molar ratios can be calculated and shown in Table S1.

Table S1. The volume, molar ratio of 0D and 3D perovskite for the 12 samples and the concentration correction coefficient of 12 samples.

Volume of 3D (uL)	Volume of 0D (uL)	Molar ratio of 0D:3D	Volume of solvent (uL)	Total volume (uL)	Correction coefficient
50	50	0.04:1	4000	4100	1
50	100	0.08:1	4000	4150	1.01
50	150	0.12:1	4000	4200	1.02
50	200	0.16:1	4000	4250	1.03
50	250	0.2:1	4000	4300	1.05
50	300	0.24:1	4000	4350	1.06
50	400	0.32:1	4000	4450	1.08
50	500	0.4:1	4000	4550	1.11
50	600	0.48:1	4000	4650	1.13
50	700	0.56:1	4000	4750	1.16
50	800	0.64:1	4000	4850	1.18
50	1000	0.8:1	4000	5050	1.23

Table S2. The peak position and QY of samples with different ratio of $Cs_4PbBr_6/CsPbCl_3$.

Sample ($Cs_4PbBr_6/CsPbCl_3$ ratio)	Peak position (nm)	QY (%)
0.04:1	434	55
0.08:1	441	58
0.12:1	447	64
0.16:1	450	75
0.2:1	456	86
0.24:1	463	90
0.32:1	467	92
0.4:1	475	93
0.48:1	478	93
0.56:1	483	95
0.64:1	486	95
0.8:1	491	95

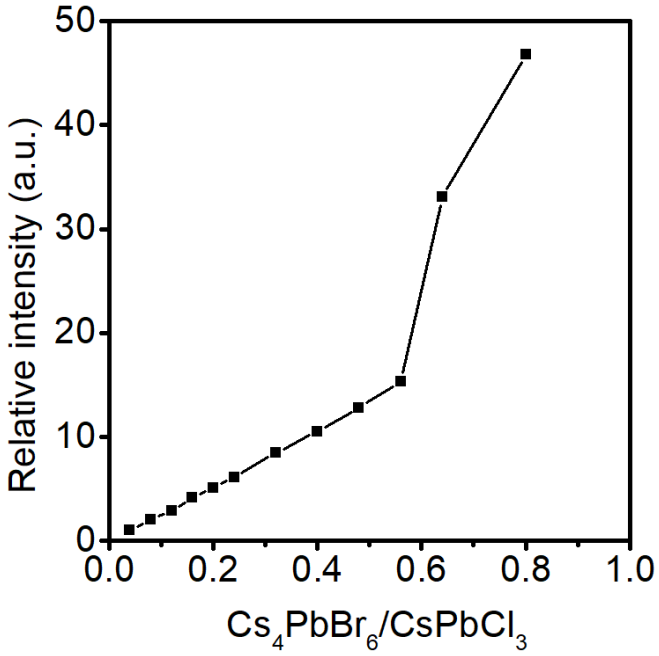

Figure S1. Relative absorption intensity along with the different ratio of $Cs_4PbBr_6/CsPbCl_3$. (the x-axis is the molar ratio of 0D:3D; the y-axis is absorbance intensity at 314 nm of others compared with the initial intensity of 0D:3D=0.04:1 and the absorbance intensity at 314 nm of 0D:3D=0.04:1 is set as the standard value)

We can estimate the amount of 0D perovskite NCs in all the products by comparing their intensities of 314nm with the initial intensity of 0D:3D=0.04:1 in their absorption spectra. In this process, we assume that the concentrations of 3D perovskite NCs remain constant. However, small deviation may be introduced due to the declining concentration of 3D perovskite. With increasing the volume of 0D perovskite, the whole volume of the solution will increase which will cause the concentration of 3D perovskite NCs to decline. For example, with 100 uL adding, the whole volume of the solution becomes 4150 uL. The concentration of 3D perovskite NCs declines compared to the initial concentration (4100 uL). Hence, another 11 absorbance spectra were multiplied a coefficient to remove the impacts of concentration. Similarly, the initial coefficient of 0D:3D=0.04:1 was set as 1. The other coefficients can be calculated by dividing their volume by 4100 (Table S1). After corrected by these coefficients, the spectrum used to show the variation of 0D perovskite NCs will be more precise.

The absorption peak increases linearity as the increase of the content of 0D perovskite. Further increasing the content of 0D perovskite, the absorption peak increases suddenly. This is because when too many 0D perovskite introduced, the ratio of 3D perovskite is small. And for the absorption measurement, we take 0.1ml out to perform the test. The error maybe too large. This can be confirmed by the TEM image, where few 3D perovskite NCs can be found in the product.

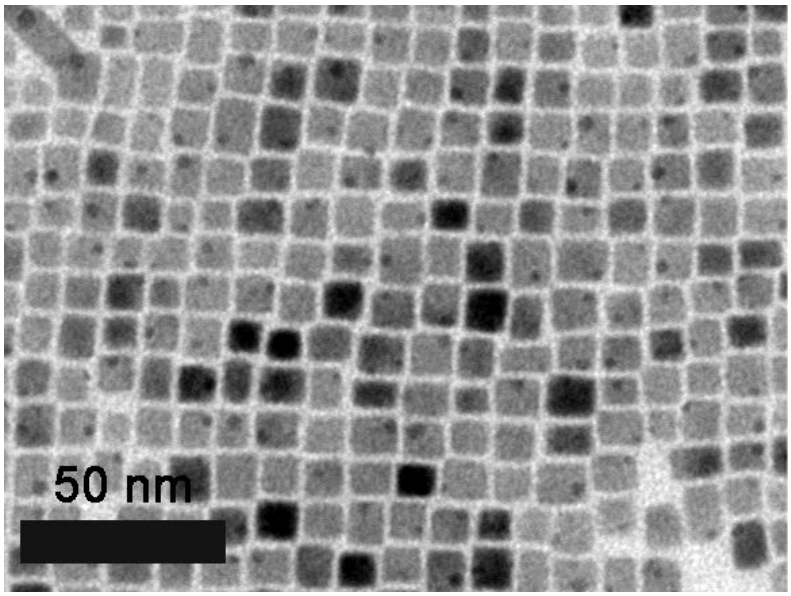

Figure S2. TEM image of $CsPbCl_3$ NCs.

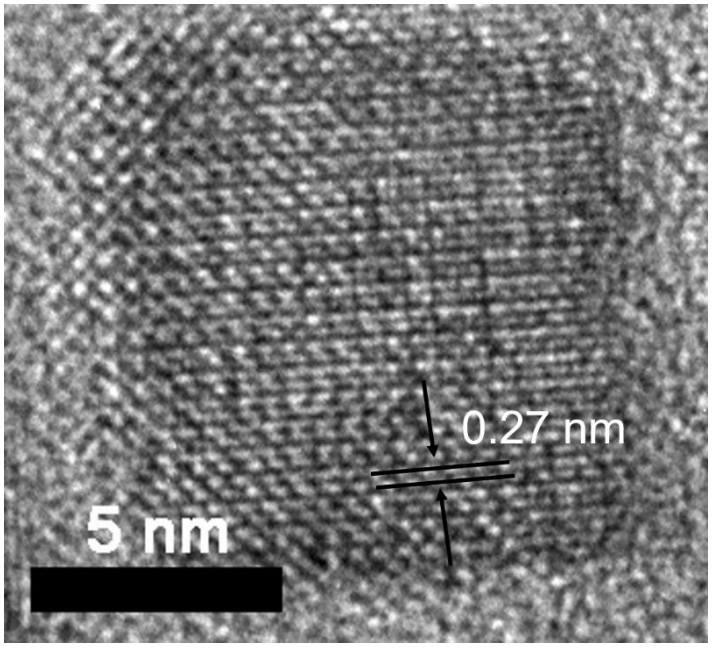

Figure S3. HRTEM image of $CsPbCl_3$ NCs.

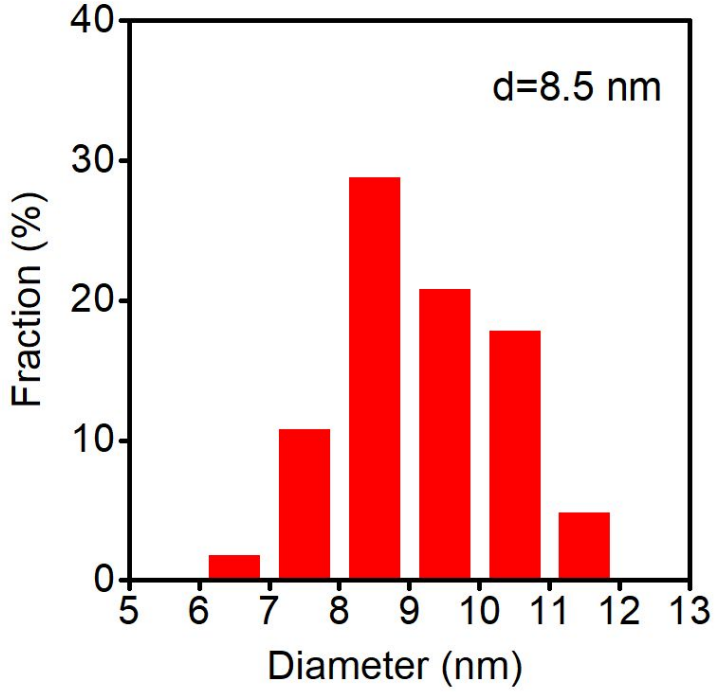

Figure S4. The size distribution of $CsPbCl_3$ NCs.

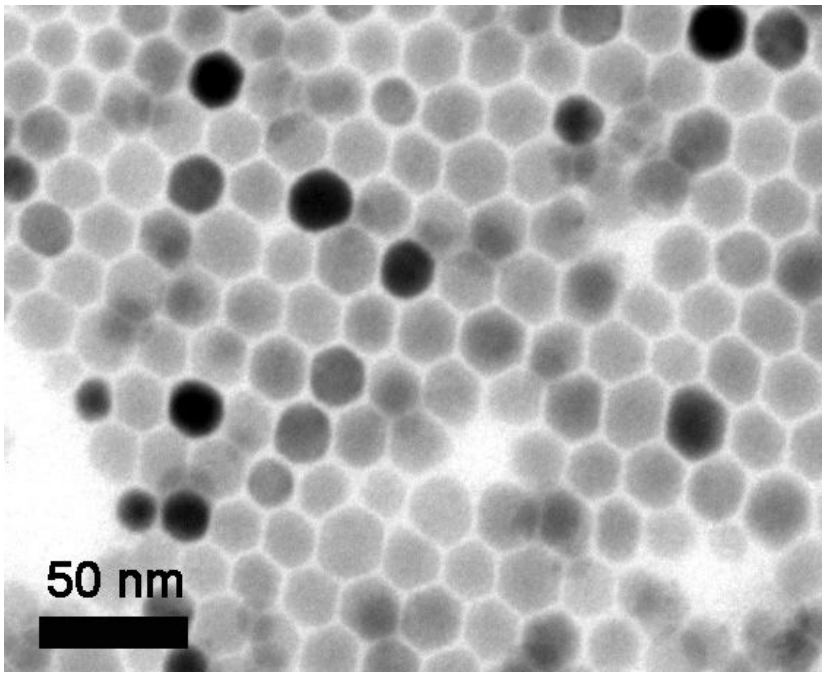

Figure S5. TEM image of Cs_4PbBr_6 NCs.

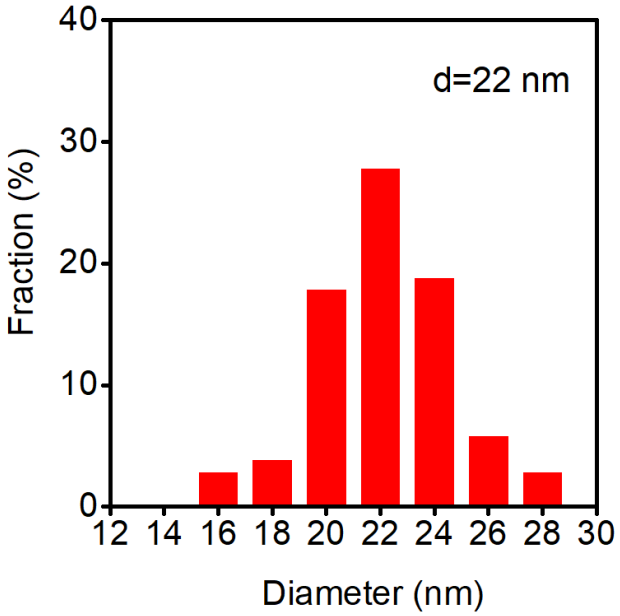

Figure S6. The size distribution of Cs_4PbBr_6 NCs.

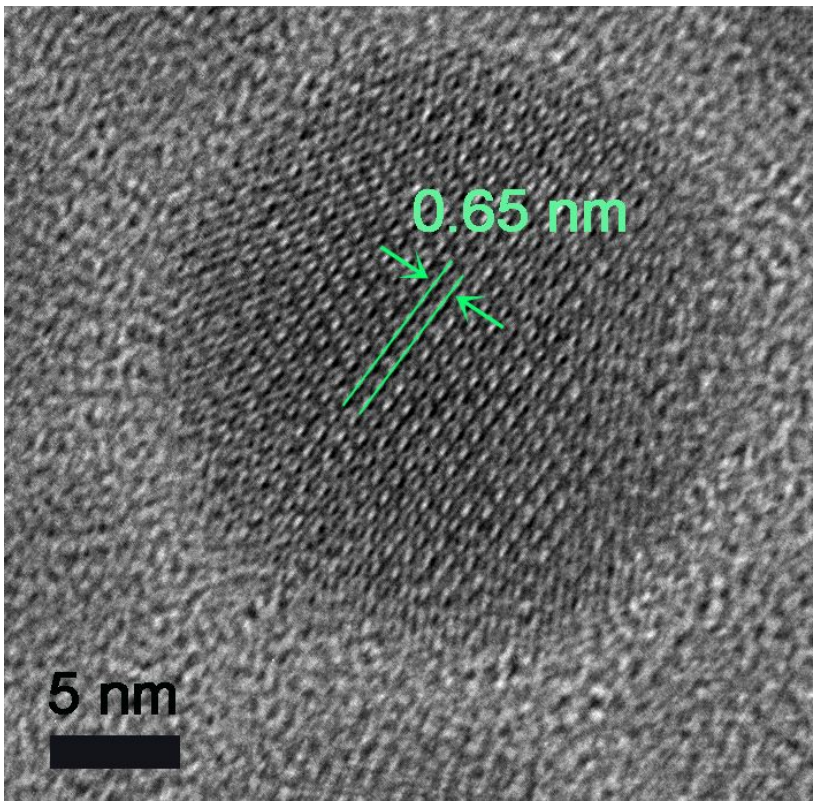

Figure S7. HRTEM image of the $Cs_4Pb(Cl/Br)_6$ from S2.

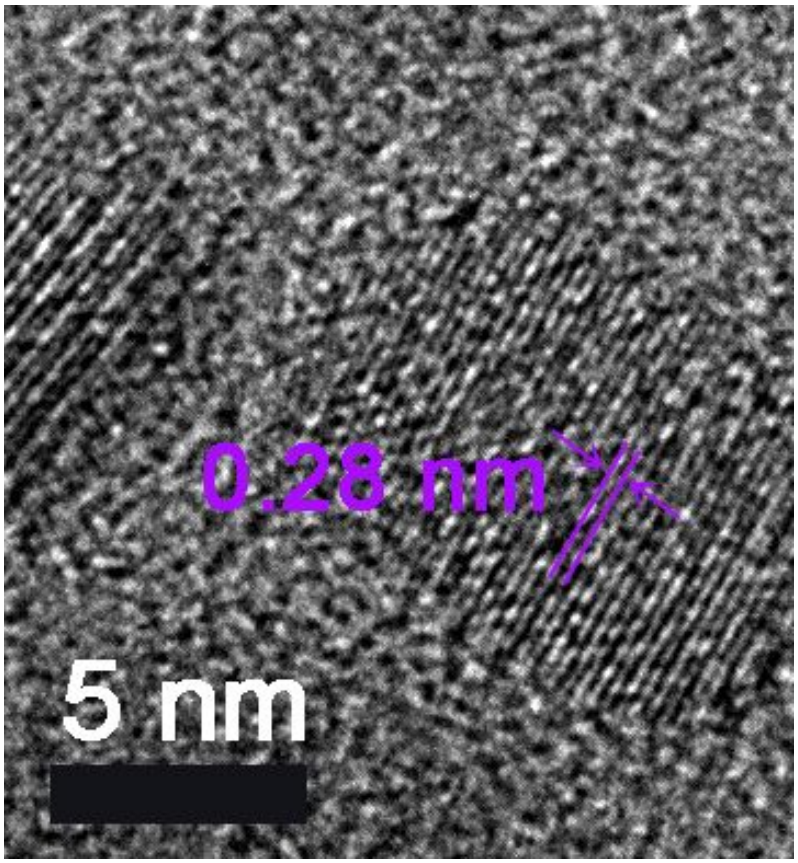

Figure S8. HRTEM image of the $CsPb(Cl/Br)_3$ from S2.

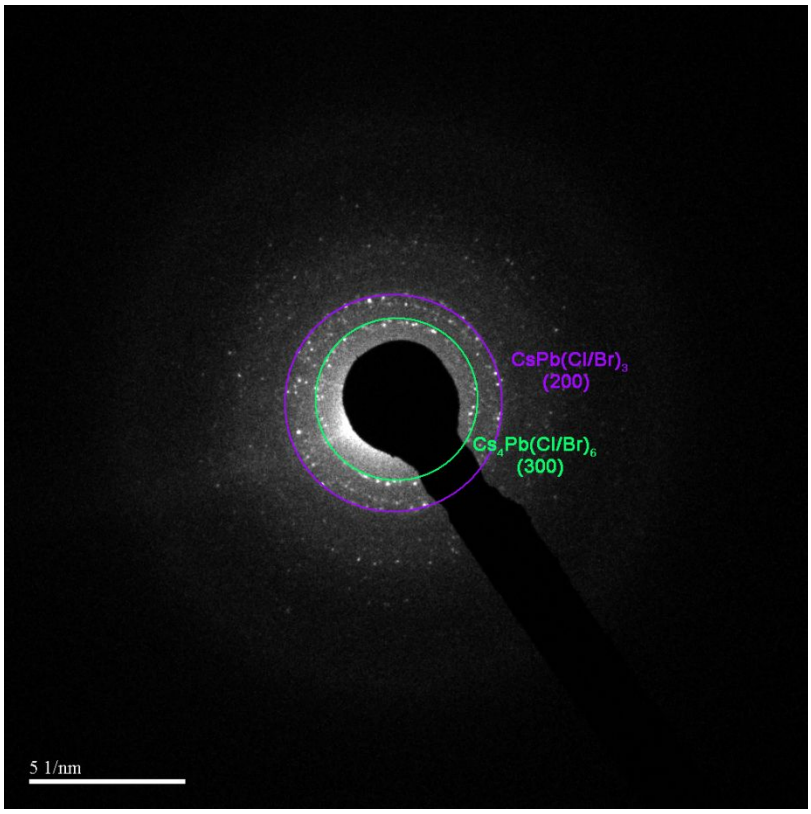

Figure S9. SAED pattern of the sample S2.

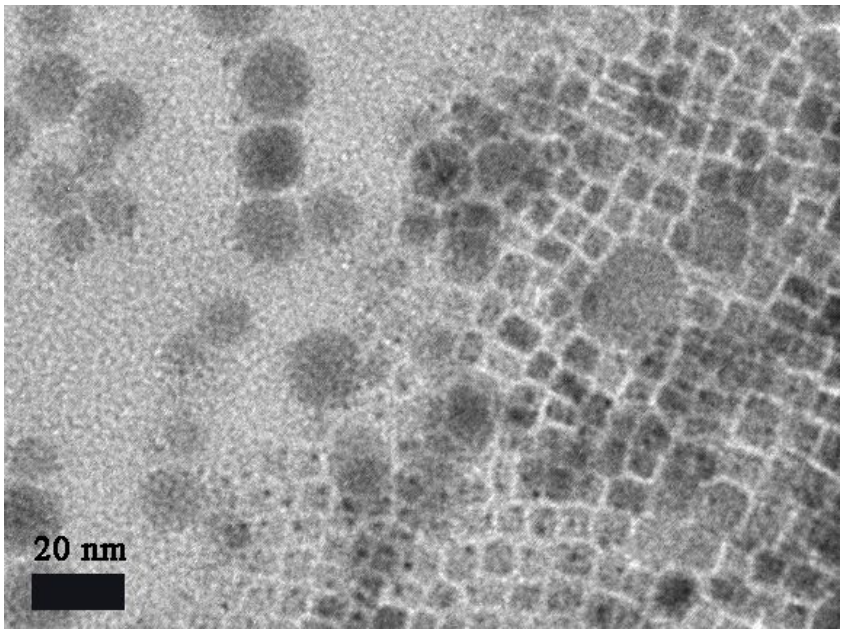

Figure S10. TEM image of the sample S1.

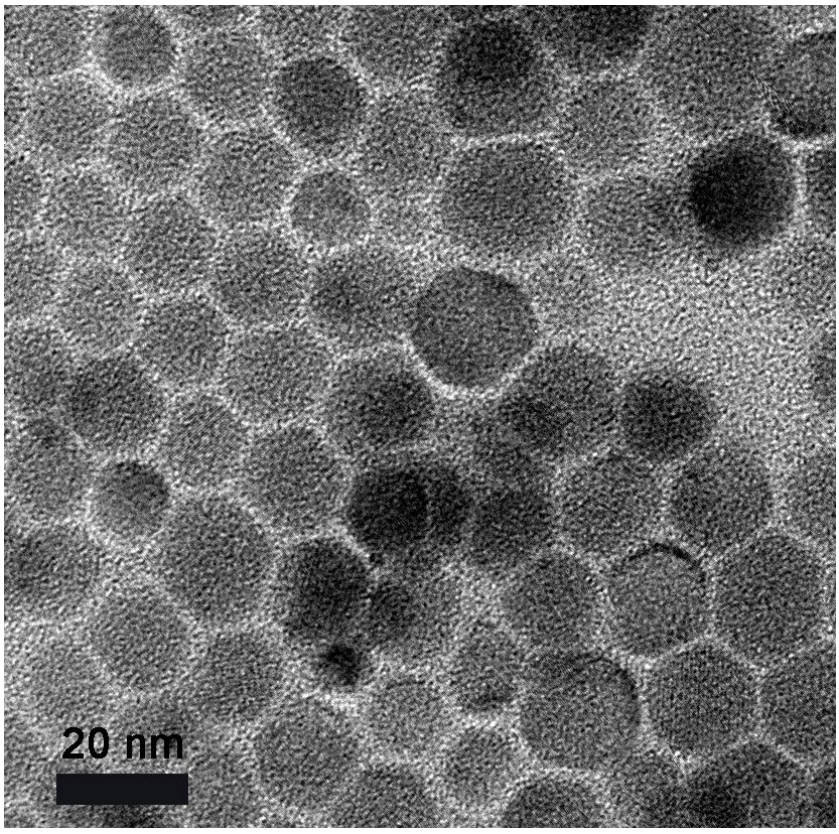

Figure S11. TEM image of the sample S3.

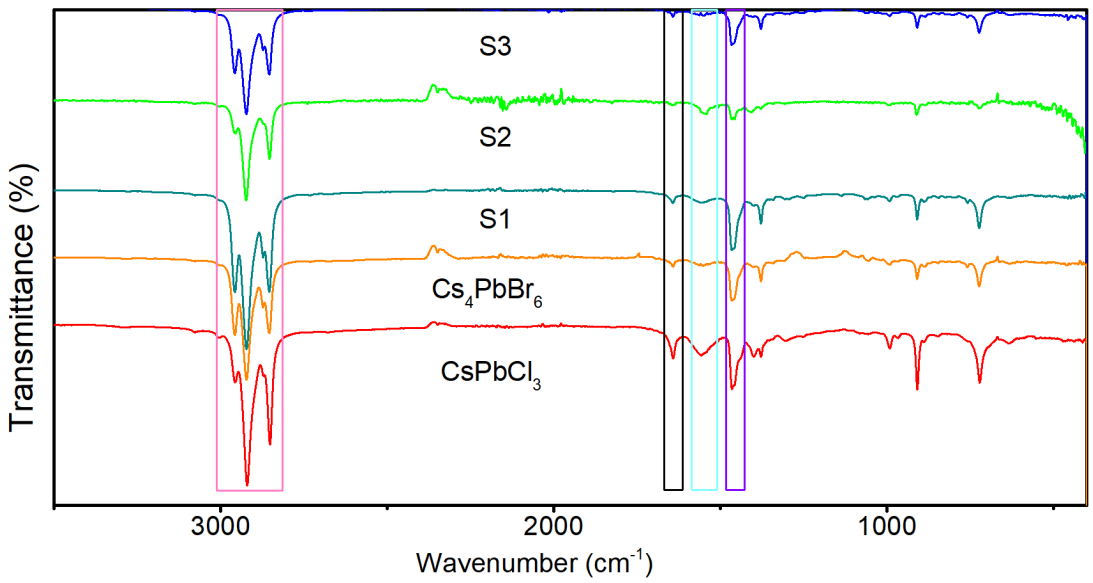

Figure S12. FTIR spectra of S1-S3, Cs_4PbBr_6 and $CsPbCl_3$.

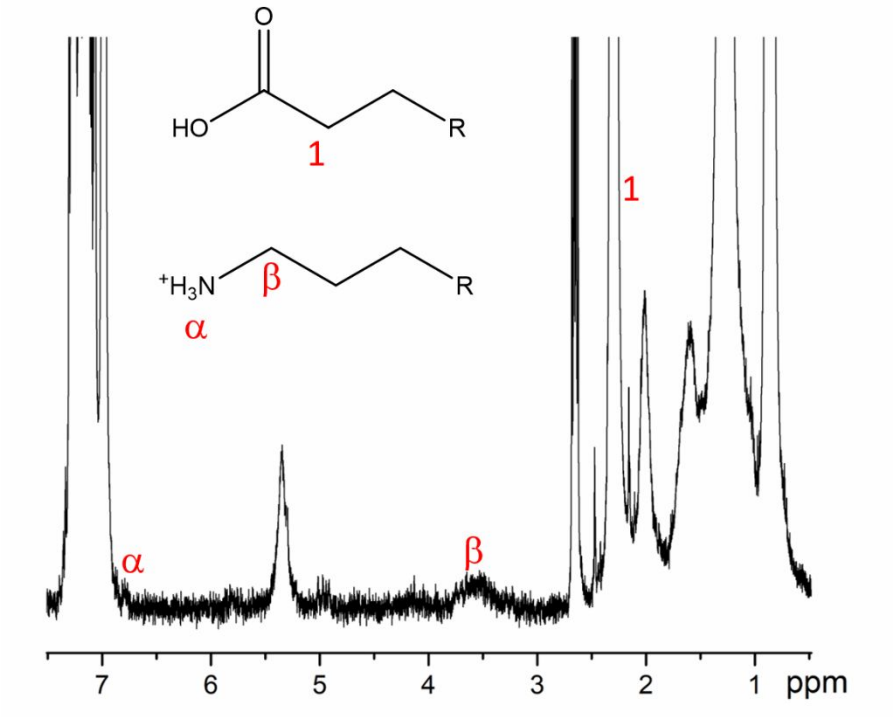

Figure S13. 1H NMR spectrum of Sample S2.

Calculation of Radiative & non-radiative decay rate.

The average PL lifetime: $\tau_{avg} = \sum f_i \times \tau i$ (i=1, 2, 3) (S1)

Radiative lifetime: $\tau_r = \frac{\tau_{avg}}{QY}$ (S2)

Nonradiative lifetime: $\tau_{nr} = \frac{\tau_{avg}}{1 - QY}$ (S3)

Radiative decay rate: $k_r = \frac{1}{\tau_r}$ (S4)

Nonradiative decay rate: $k_{nr} = \frac{1}{\tau_{nr}}$ (S5)

Table S3. PL lifetimes average lifetime (τ_{avg}), QY, radiative decay rate (k_r), apparent nonradiative decay rate (k_{nr}) of S1, S2, S3 and their couterparts by hot injection (HI) method.

Sample	f_1 (%)	f_2 (%)	τ_1 (ns)	τ_2 (ns)	τ_{avg} (ns)	QY (%)	k_r (ns^{-1})	k_{nr} (ns^{-1})
434 nm HI	41	59	1.4	8.9	5.8	12	0.02	0.15
434 nm S1	67	33	1.3	7.3	3.3	55	0.16	0.13
463 nm HI	31	69	1.2	8.5	6.2	30	0.05	0.11
463 nm S2	45	55	1.7	5.0	3.6	90	0.25	0.02
486 nm HI	26	74	1.9	8.9	7.1	58	0.08	0.06
486 nm S3	70	30	2.6	6.9	3.9	95	0.24	0.01

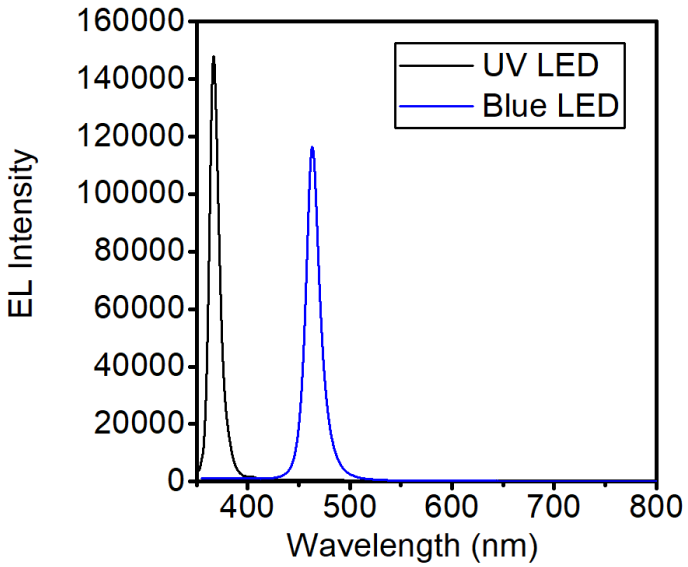

Figure S14. EL spectra of LED before and after coating with NCs at the same driving current.

After coating with the NCs, the peak of 365 nm totally disappears while the peak of 463 nm shows up. Besides, the peak intensity of 463 nm can be compared to the original intensity of 365 nm, indicating the effectiveness of light conversion.

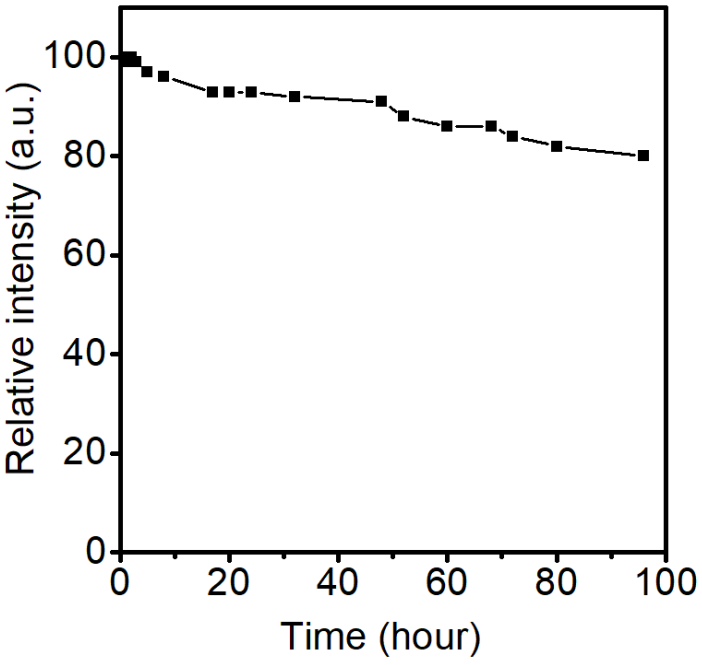

Figure S15. The stability test of the blue emitting LED.

The blue emitting LED possess excellent stability, which can maintain 80 % of the original after continues working 90 hours.

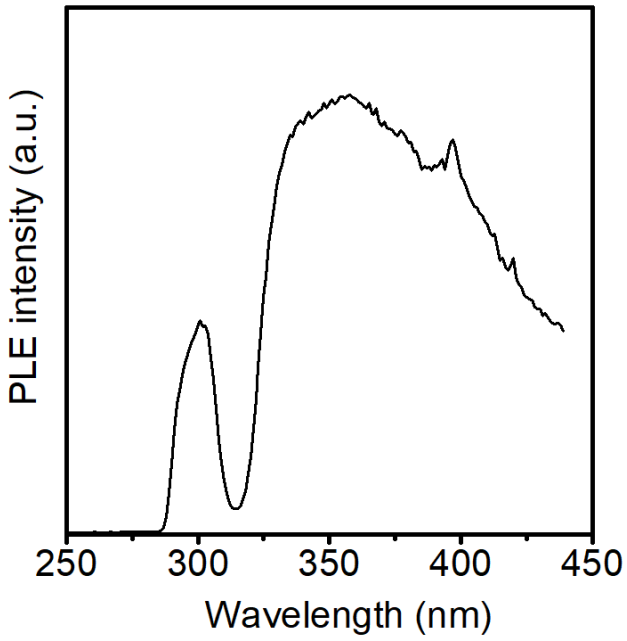

Figure S16. PLE spectrum of sample S2 (detected at 463 nm).

As can be seen from this figure, a sharp dip at 314 nm can be observed while a sharp peak in the absorption spectrum is found at the same wavelength. However, $Cs_4Pb(Cl/Br)_6$ exhibits very strong absorption at 314 nm. Therefore, it is reasonable to speculate that the strong PL peak of the composites originate from $CsPb(Cl/Br)_3$ NCs.

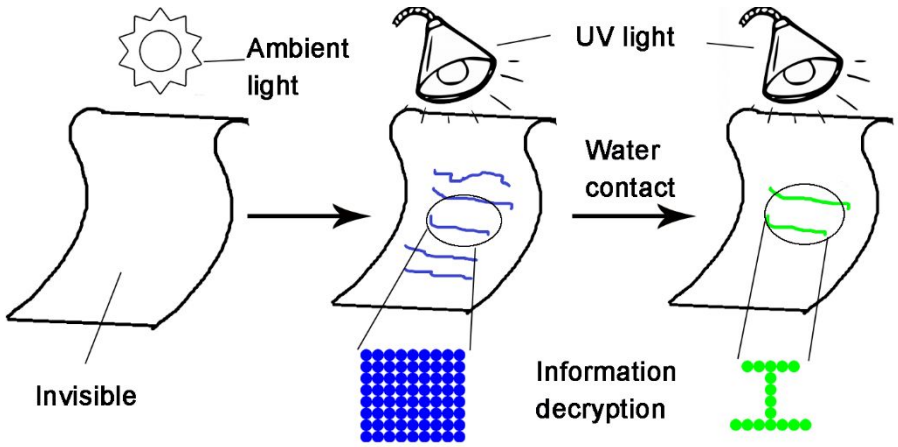

Scheme S1. Schematic illustration of information encryption and decryption process.

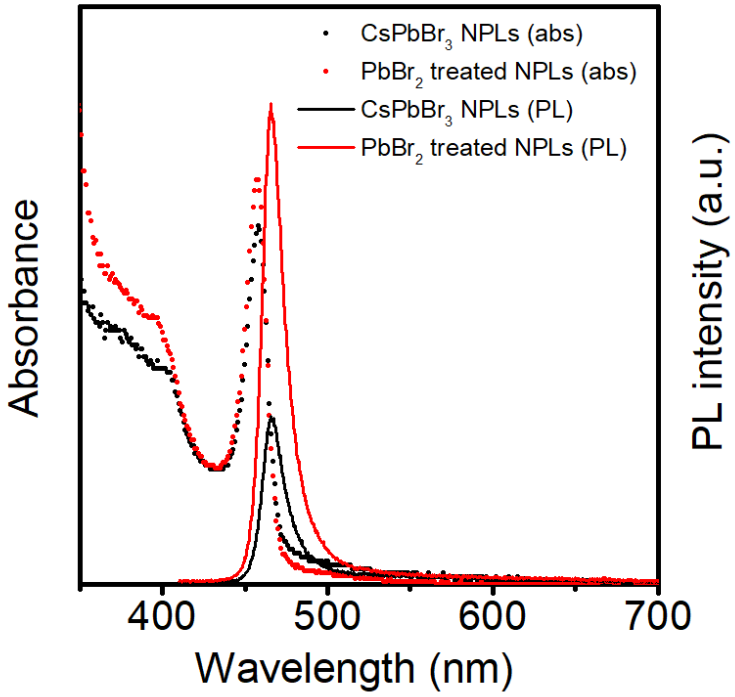

Figure S17. UV/Vis absorption and PL spectra of $CsPbBr_3$ NPLs and $PbBr_2$ treated NPLs.

The PL and absorption peaks are nearly no change after $PbBr_2$ treated $CsPbBr_3$ NPLs.

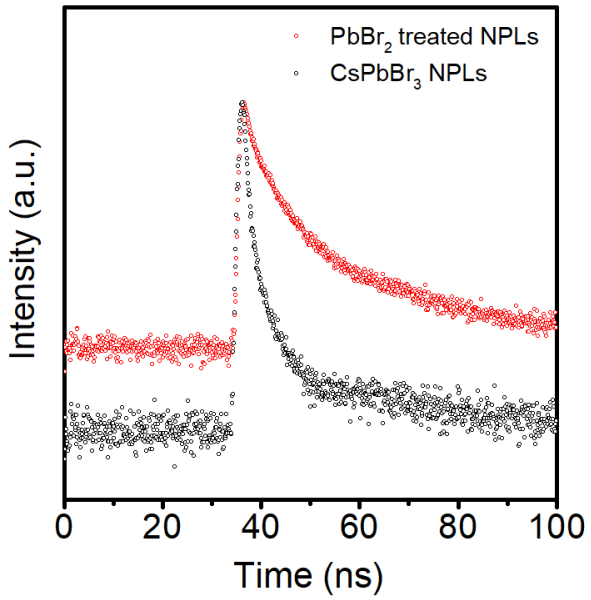

Figure S18. PL decay curves of $CsPbBr_3$ NPLs and $PbBr_2$ treated NPLs.

Table S4. PL lifetimes average lifetime (τ_{avg}), QY, radiative decay rate (k_r), apparent nonradiative decay rate (k_{nr}) of $CsPbBr_3$ NPLs and $PbBr_2$ treated NPLs.

Sample	f_1 (%)	f_2 (%)	τ_1 (ns)	τ_2 (ns)	τ_{avg} (ns)	QY (%)	k_r (ns^{-1})	k_{nr} (ns^{-1})
$CsPbBr_3$ NPLs	56	44	1.03	6.95	3.63	31	0.08	0.19
$PbBr_2$ treated NPLs	19.7	80.3	2.3	11.9	9.98	85	0.08	0.02

After $PbBr_2$ treated, the PL QY of $CsPbBr_3$ NPLs is improved and the nonradiative decay rate is reduced from 0.19 ns^{-1} to 0.02 ns^{-1}.

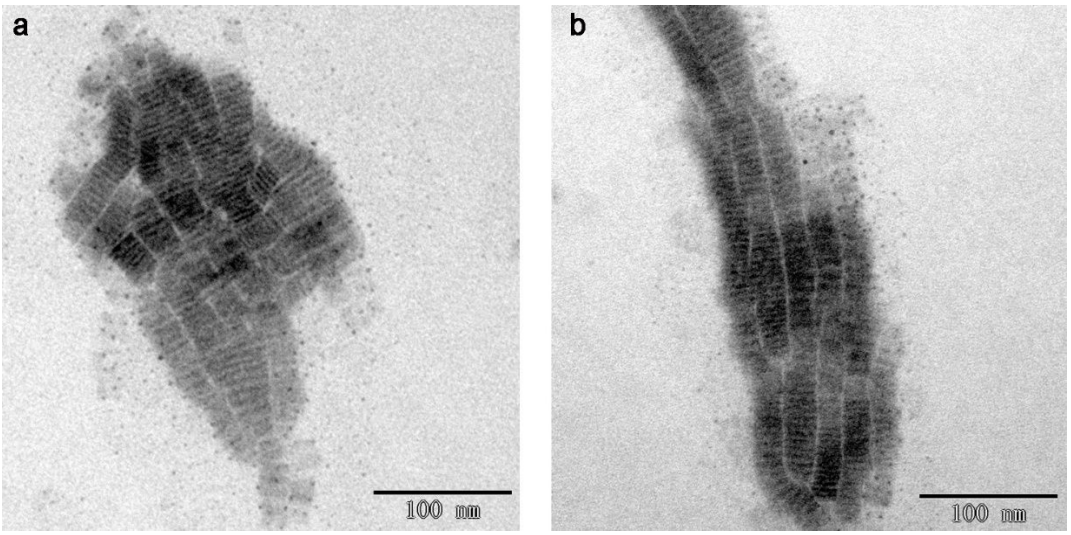

Figure S19. TEM images of $CsPbBr_3$ NPLs (a) and $PbBr_2$ treated NPLs (b).

The morphology of the NPLs and their thickness are virtually unchanged after the $PbBr_2$ treated.

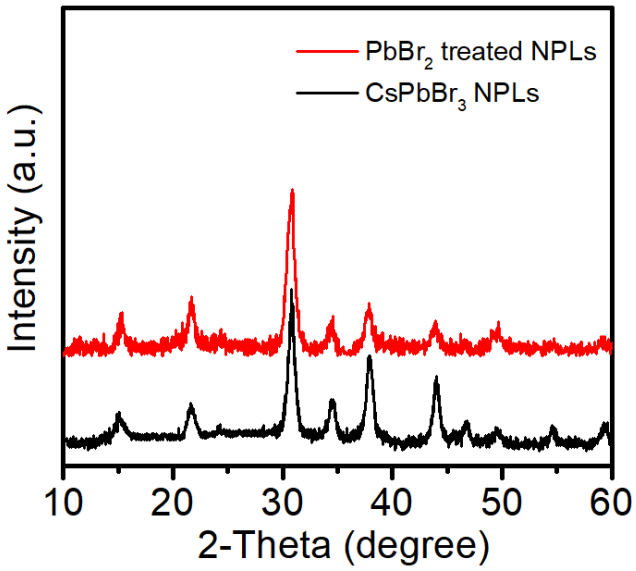

Figure S20. XRD patterns of $CsPbBr_3$ NPLs and $PbBr_2$ treated NPLs.

As can be seen from this figure, all the peaks do not change noticeably, suggesting that the crystal structure remains the same after the addition of the $PbBr_2$.

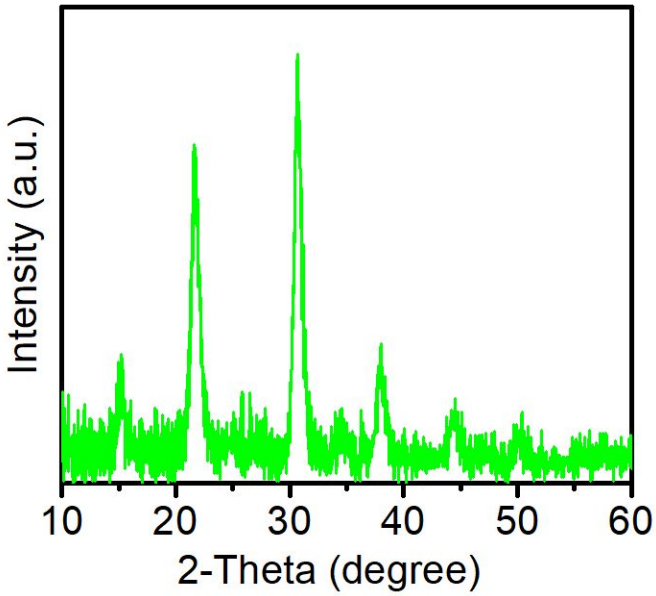

Figure S21. XRD pattern of sample S2 after water treatment.
The transformation process can be written as:

$$Cs_4PbBr_6 \rightarrow CsPbBr_3 + 3CsBr_{(water)} \quad \text{(S1)}$$

Figure S22. Security application using the number “888”.

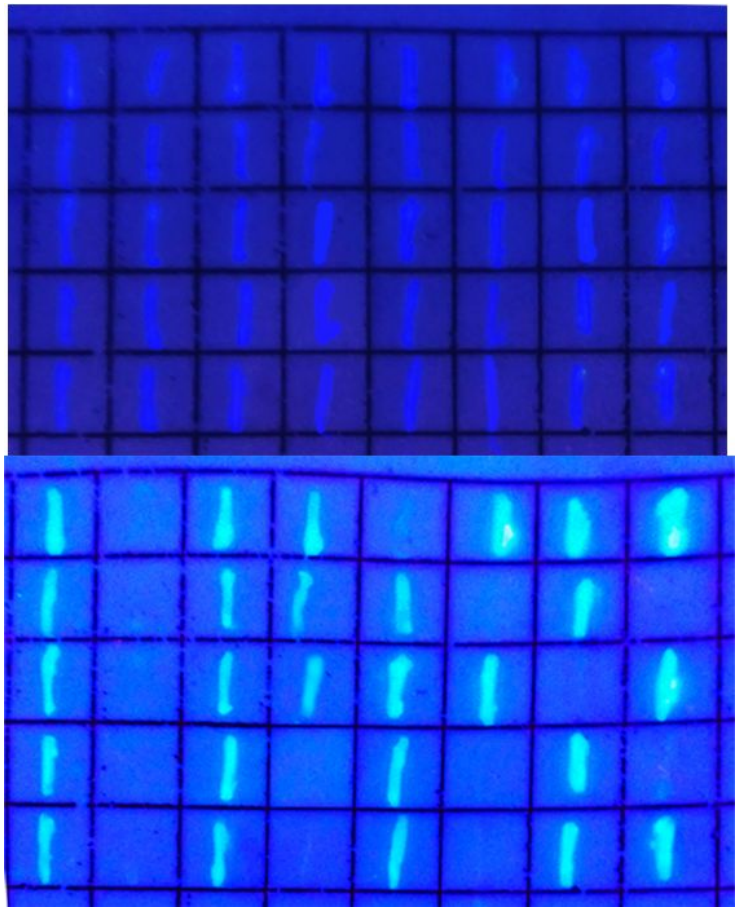

Figure S23. Security application using binary-coded microarray data.

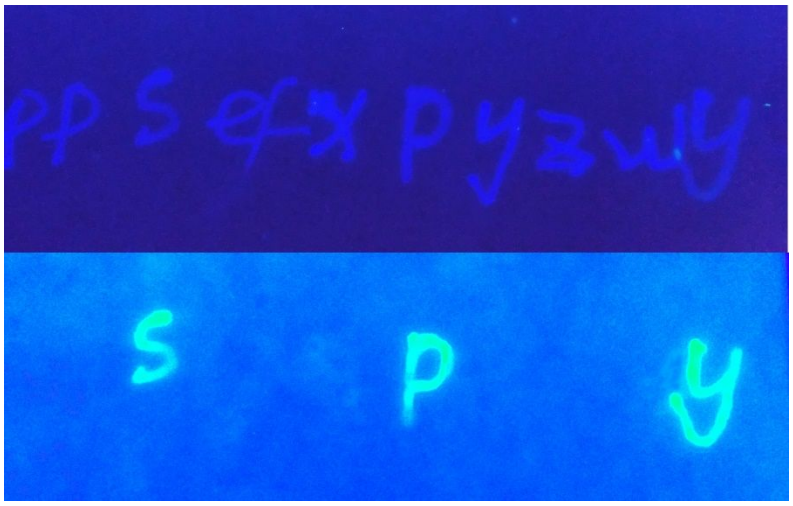

Figure S24. Security application of English characters.

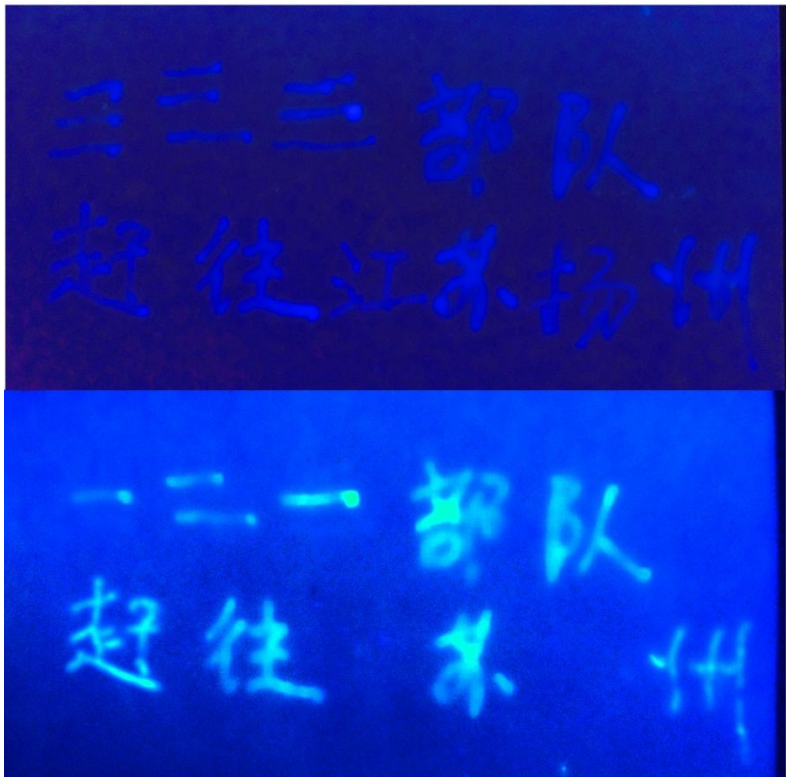

Figure S25. Security application using Chinese characters.

Figure S26. The weather painting written by security inks under UV light and decryption information of the patterns after treated with water.

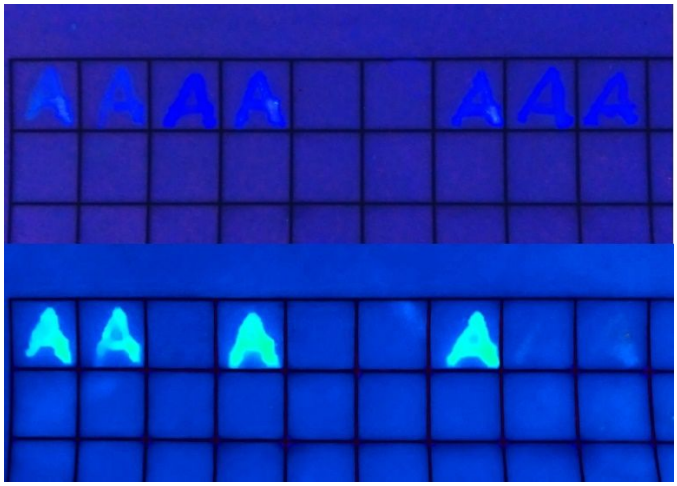

Figure S27. Security application of Morse-coded microarray data storage chips.

Reference

(1) Velázquez, M.; Ferrier, A.; Péchev, S.; Gravereau, P.; Chaminade, J.-P.; Portier, X.; Moncorgé, R. Growth and Characterization of Pure and Pr3+-Doped Cs4pbbr6 Crystals. J. Cryst. Growth 2008, 310, 5458-5463.

(2) Liu, Z.; Peters, J. A.; Stoumpos, C. C.; Sebastian, M.; Wessels, B. W.; Im, J.; Freeman, A. J.; Kanatzidis, M. G. Heavy Metal Ternary Halides for Room-Temperature X-Ray and Gamma-Ray Detection. SPIE: 2013; Vol. 8852.